Machine learning and computer vision based quantification of cell number in MRI-based cell tracking

Muhammed Jamal Afridi[1], Matt Latourette[2], Margaret F Bennewitz[3], Arun Ross[1], Xiaoming Liu[1], and Erik M Shapiro[2]

[1]Department of Computer Science and Engineering, Michigan State University, East Lansing, MI, United States, [2]Department of Radiology, Michigan State University, East Lansing, MI, United States, [3]Vascular Medicine Institute, University of Pittsburgh, Pittsburgh, PA, United States

INTRODUCTION: MRI detection of single cells[1] is an underutilized advancement in MRI-based cell tracking. One reason for its underutilization has been a lack of methods for quantifying information in these images. For example, single cell detection enables quantification of cell numbers and accurate localization of cell location. To achieve single cell detection by MRI, cells are labeled with superparamagnetic iron oxide particles allowing their detection as punctate hypointensities in T2*-weighted MRI. We have developed a machine learning and computer vision based strategy for the generalizable detection and quantification of MRI-based single cell detection. Experimental results show that our approach can detect spots with an accuracy of 99.8%

METHODS: Agarose phantoms were constructed with a dilute, known number of 4.5 micron diameter MPIOs from Dynal. Each bead has 10 pg of iron, simulating a labeled cell. We performed MRI of the agarose phantom at 7T using a 3D FLASH sequence with TR/TE=30/5-20ms, and 100 µm or 200 µm isotropic voxels (Figure 1). We explain our learning based approach in a stepwise manner:

(1) We first create a 3D model of the spots using superpixels[2]. Visually, a hypointense spot appears as a cluster of *3*D pixels with high variations in its *3*D shape and intensity, wrapped inside a cover of background pixels as conceptually illustrated in Fig. 2. The high variability in the shape of the hypointensity is well described in Zabow, et al[3] and is due to the location of the magnetic material within a voxel. The darker region represents the interior of a spot, containing hypointense contrast from the cells, whereas the surrounding yellow shows its exterior (background pixels). To precisely model such cross-sections, we generate superpixels in the 2D slices, as shown in Fig. 3. A superpixel groups local pixels with similar intensities into one unit. Therefore, interior and exterior pixels are precisely kept in separate superpixels irrespective of their shapes and sizes. Interior and exterior superpixels in consecutive slices of MRI can then be respectively connected to form a 3D spot model. This approach allows our final classification to be performed on the groups of superpixels rather than at pixel level and hence significantly reduce the size of testing samples.

(2) To learn a classification model that can accurately differentiate between true spots and non-spots, we first collect ground truth spot labels by asking a human labeler to mouse-click on the dark spots contained in 2D slices of MRI.

(3) For every 3D spot model, a set of features are extracted that can be used later by a learnt classifier to classify it as a spot or not. Considering that non-spot models can be in hundreds of thousands, we base our features on computationally efficient operations. Therefore, we utilize the intensity differences of the interior of a spots with its exterior for computing features.

(4) Once features are extracted, we use a feature selection algorithm to select the most useful subset of the features, in order to get rid of the redundant and irrelevant ones. This allows the classifier to focus learning on the effective feature only and hence increases accuracy. Finally, a team of classifiers is collectively learned on the training feature set to classify candidate models as spots or not spots in the testing set.

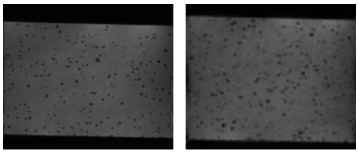

Figure 1: Slice at 100 µm (left) and 200 µm (Right)

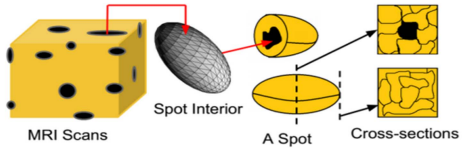

Figure 2: Conceptualizing the spot model

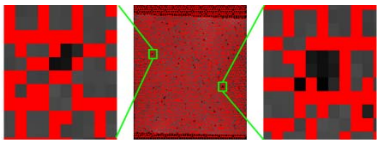

Figure 3: Superpixels on real image (orange=boundary)

RESULTS AND DISCUSSION: Based on the manual spot labeling, we observed 5404 spots in a total of 86 labeled slices of MRI with 366,061generated non-spot models in these slices. We split these slices into two halves. We used the first half as a training set and the second half for testing. We used the area under the curve (AUC) as a measure to evaluate the performance of the learnt model. Our approach can detect with an AUC of 99.8% as displayed by the green curve in Fig. 4. Secondly, we also investigate how *much* the performance will decrease if we decrease the resolution. When we reduce the resolution from 100 µm to 200 µm, the system still achieves an accuracy of 96.6%, as indicated by the red curve in Fig. 4. We show some detected spots by our algorithm in Fig. 5. Further, with two additional algorithmic advancements, we evaluate our approach on the in vivo brain MRI of two rats with cells transplanted into them. One rat's brain MRI is used for learning the classifier whereas the other rat's brain MRI data is used for testing. Human labels of the spots were obtained in the same manner on both sets. On the testing set, there are 2,296 labeled true spots, and 3,750,695 potential non spots (anywhere that is not labeled is a non spot). Our system correctly classifies all non spots, while falsely classifies 388 true spots as non spots, which has an in vivo spot detection accuracy of 99.99%. This is an impressive result considering the huge amount of non spots our classifier has to suppress. Our ongoing work is to further improve the in vivo accuracy, especially for lower-resolution MRI scans.

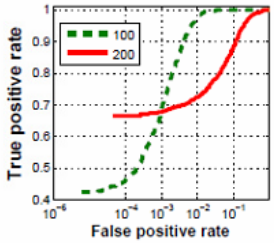

Figure 4: (a) AUC with different Resolutions

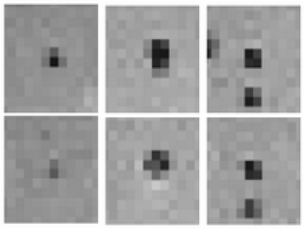

Figure 5: Each column is a spot of length=2 slices

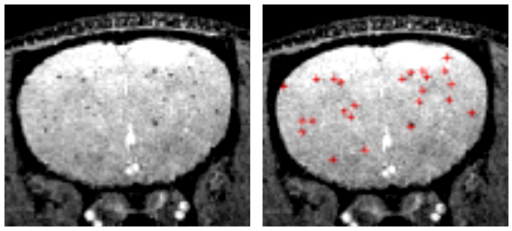

Figure 6: Rat brain MRI (left), Human labeling on slice (Right)

CONCLUSIONS: This is the first systematic study to develop advanced data-driven machine learning and computer vision algorithms for the automated detection of magnetically labeled cells in MRI images. When the algorithm was compared to manually labeled spots in tube data, the AUC is 99.8% with 100 µm isotropic voxels, with a decrease to 96.6% for 200 µm voxels. With two additional algorithmic advancements, this approach can also be adapted to rats' brain MRI data acquired in vivo and achieve a detection accuracy of 99.99%. **Refs: 1)** Shapiro, et al, MRM 2005 **2)** Li, et al, CVPR 2012 **3)** Zabow, et al, MRM 2011.